Larger spatial footprint of wintertime total precipitation extremes in a warmer climate

Article

Published Version

It is advisable to refer to the publisher's version if you intend to cite from the work. See Guidance on citing.

Larger Spatial Footprint of Wintertime Total Precipitation Extremes in a Warmer Climate

Emanuele Bevacqua[1,2] , Theodore G. Shepherd[1] , Peter A. G. Watson[3], Sarah Sparrow[4] , David Wallom[4] , and Dann Mitchell[3,5]

[1]Department of Meteorology, University of Reading, Reading, UK, [2]Now at Helmholtz Centre for Environmental Research—UFZ, Leipzig, Germany, [3]School of Geographical Sciences, University of Bristol, Bristol, UK, [4]Oxford e-Research Centre, Engineering Science, University of Oxford, Oxford, UK, [5]Cabot Institute for the Environment, University of Bristol, Bristol, UK

Abstract The simultaneous occurrence of extremely wet winters at multiple locations in the same region can contribute to widespread flooding and associated socio-economic losses. However, the spatial extent of precipitation extremes (i.e., the area in which nearby locations experience precipitation extremes simultaneously) and its future changes are largely overlooked in climate assessments. Employing new multi-thousand-year climate model simulations, we show that under both 2.0 °C and 1.5 °C warming scenarios, wintertime total precipitation extreme extents would increase over about 80%–90% of the Northern Hemisphere extratropics (i.e., of the latitude band 28°–78°N). Stabilizing at 1.5 °C rather than 2.0 °C would reduce the average magnitude of the increase by 1.7–2 times. According to the climate model, the increased extents are caused by increases in precipitation intensity rather than changes in the spatial organization of the events. Relatively small percentage increases in precipitation intensities (e.g., by 4%) can drive disproportionately larger, by 1–2 orders of magnitude, growth in the spatial extents (by 93%).

Plain Language Summary One of the most impact-relevant and studied effects of global warming is the intensification of precipitation extremes. When extremely wet winters occur simultaneously at multiple locations within the same region, their cumulative impacts can be particularly high and enhanced as a result of limited resources available to cope with simultaneous damages. Despite the impacts caused by widespread extremes, climate change studies have typically disregarded the spatial extension of the extremes. Here, based on new multi-thousand-year climate model simulations, we show that—over most of the Northern Hemisphere extratropics, that is, most of the latitude band 28°–78°N—the spatial footprint of total wintertime precipitation extremes is projected to largely widen in the future. This widening results from a warmer, and therefore moister, atmosphere that will intensify precipitation. Holding global warming to 1.5 °C rather than 2.0 °C, in line with the Paris Agreement, would be beneficial to society as it could limit the average increase in the extension over the Northern Hemisphere extratropics by up to a factor of 2. To develop better preparedness for such extreme events, stakeholders should consider that a small increase in precipitation intensities (for example, by 4%) could result in large (by 93%) increases in spatial extent.

1. Introduction

Extremely wet winters resulting from one or multiple precipitation events can contribute to flooding leading to severe societal, natural, and economic impacts. When such extremely wet conditions occur simultaneously at multiple locations within the same region, their impacts may be enhanced and lead to extreme cumulative losses (Leonard et al., 2014). In fact, widespread extreme events can affect the ability of governments and international (re-)insurance companies to respond to the emergency, given that resources and funds need to be provided at multiple locations and industrial sectors simultaneously (Enríquez et al., 2020; Kemter et al., 2020; Zscheischler et al., 2020). Recent extreme events showed that, as a result of persistent atmospheric conditions, extremely wet winters and associated flooding can affect multiple countries simultaneously and put high pressure on railway/road networks and transnational risk-reduction mechanisms (Jongman et al., 2014; Zscheischler et al., 2020). For example, the extremely wet winter of 2013/2014 in southern England, Wales, Ireland, and southern Norway led to major disruptions to transport

and damages to livelihoods and infrastructure, and is estimated to have caused hundreds of millions of pounds of insured losses (Kendon & McCarthy, 2015; Schaller et al., 2016). Recently, Berghuijs et al. (2019) found that the spatial extent of synchronous river flooding in Europe has increased during the last decades, although it was not demonstrated that anthropogenic climate change contributed to the increase (Kemter et al., 2020).

Despite the relevance of the spatial extent of precipitation extremes for flooding-related impacts, studies have focused mainly on assessing the changes in the magnitude of the local precipitation extremes (Hoegh-Guldberg et al., 2018). In a future warmer climate, a moister atmosphere will favor higher precipitation magnitudes, while changes in the atmospheric circulation, for example, storm track variations, may modulate both precipitation magnitudes and spatial patterns (e.g., Bevacqua, Zappa, et al., 2020; O'Gorman & Schneider, 2009). As a result, these mechanisms may change the spatial extent of seasonal precipitation extremes. Changes in the spatial extent of precipitation events at the synoptic time scale (e.g., hourly and daily) have been investigated over different regions employing a range of methods (Chang et al., 2016; Dwyer & O'Gorman, 2017; Guinard et al., 2015; Nikumbh et al., 2019; Touma et al., 2018; Wasko et al., 2016). To the best of our knowledge, the extent of wintertime total precipitation extreme events (i.e., the area in which nearby locations experience total precipitation extremes in the same season) and its projected change under anthropogenic global warming has not yet been investigated.

Here, we close this research gap, focusing on precipitation in the Northern Hemisphere extratropics. Specifically, we assess the present-day extent of the wintertime total precipitation events and the future changes under 1.5 °C and 2.0 °C warming scenarios, including an investigation and discussion of the drivers of the changes. A large sample size of data is required to analyze extremes of this type of *spatially compounding event*, therefore we employ new multi-thousand-year climate model simulations.

2. Data and Methods

2.1. Data

We employ the citizen-science project climate*prediction*.net, which uses volunteers' personal computers, to simulate 1410 winters (December–February). We consider a present-day scenario (2006–2015; about 1 °C warmer than pre-industrial conditions in 1850–1900) and two future scenarios within which the world would be 1.5 °C and 2.0 °C warmer than pre-industrial conditions.

We employ data from the global model of the atmosphere and land surface HadAM4 (Williams et al., 2003) with an increased resolution and a large ensemble (Bevacqua, Watson, et al., 2020; Watson et al., 2020). It considers 38 vertical levels and has a horizontal resolution of ∼60 km at mid-latitudes (0.83° × 0.56° angular resolution), which is finer than that of many current global climate models and is sufficient for good simulation of extratropical synoptic features such as storms (Demory et al., 2014; Trzeciak et al., 2016; Watson et al., 2020). HadAM4 has a heritage to widely used earlier models in the HadAM series and, being particularly memory-efficient, can be used to obtain multi-thousand-year ensembles through running on the volunteers' personal computers (Mitchell, Davini, et al., 2017).

In this study, we employ the HAPPI experiment design introduced by Mitchell, AchutaRao, et al. (2017) (see the reference for details). In particular, simulations of the three scenarios were driven by prescribed fields of sea surface temperature (SST), sea ice concentration (SIC), greenhouse gases, and aerosol. The prescribed fields of the present-day scenario are time-dependent observations during 2006–2015. Simulations of the warmer scenarios were driven by prescribed SST and SIC fields obtained as the superposition of time-dependent present-day observations and changes of the spatial field (constant in time) derived from CMIP5 multi-model means. Greenhouse gases and aerosol are held at constant future values derived from RCP scenarios. The considered emission scenarios are those that give mean temperature increases close to 1.5 °C and 2.0 °C by 2100 when used in the CMIP5 models. Namely, the RCP2.6 emission scenario was considered for the 1.5 °C warming scenario, and a combination of RCP2.6 and RCP4.5 for 2.0 °C warming. These both give stabilized global mean temperatures by 2100. The different realization of the winter's weather was obtained via perturbing the initial conditions of each ensemble member on November 1st.

For each scenario, we build an ensemble within which each of the 10 yearly prescribed conditions during 2006–2015 is equally considered, that is, our 1410 winters consist of 141 simulations of the 10 individual winters of 2006–2015.

To assess the fidelity of the simulations for the purpose of the study we compare the results of the HadAM4 model with those obtained from ERA5 reanalysis (Hersbach et al., 2020).

2.2. Spatial Scale Extremes

We identify the occurrence of a local extreme event when the wintertime precipitation total exceeds its 10-year present-day return level (T_{occur} = 10 years; Figure S1 in the supporting information). To characterize the spatial extent of seasonal precipitation extremes, we proceed similarly to Berghuijs et al. (2019) and Kemter et al. (2020), that is, we consider the *spatial scale of synchronous wintertime precipitation extremes*, hereafter referred to as *spatial scale*. For a given winter and location of interest, the spatial scale is identified through recursively searching for the first circular area centered at the location (starting with a radius of 1 km) within which less than half of the surface is affected by simultaneous extremes. *Spatial scale extremes* (SS) are defined as the 100-year return level of the spatial scale (T_{SS} = 100 years), both for the present and warmer scenarios.

Given the large sample size of the ensemble simulations, return levels are defined empirically (van der Wiel et al., 2019) (e.g., the 10-year return level is defined as the $(1 - 1/10) \times 100$th percentile). We test the sensitivity of the changes in the spatial scale extreme to the return periods employed, that is, T_{occur} and T_{SS} (Tables S1–S5). We show results within the latitude band 28°–78°N; in order to robustly estimate the spatial scales in the northernmost and southernmost locations of this latitude band, we consider data northward of 22°S.

2.3. Statistical Significance

For any given location, we assess the projected change in expected spatial scale extremes. Such a change is considered *statistically significant* if the future return level lies outside the present-day 95% confidence interval. We estimate such a confidence interval based on resampling of the interannual variability. That is, we build 1000 data sets through randomly resampling 1410 winters (141 per year) from the originally simulated present-day data set. For each of the 1000 data sets, we compute the return level. The resulting 1000 return levels are then used to estimate the centered 95% confidence interval.

2.4. Drivers of the Changes in Spatial Scale Extremes

The multivariate probability density function (pdf) $f(P_1, ..., P_N)$ of the precipitation variables at all N locations can be decomposed into the product of the N marginal pdfs f_{P_i} of the precipitation at individual locations and the copula density c that describes the spatial dependencies in the precipitation field (Sklar, 1959). That is, $f(P_1,...,P_N) = f_{P_1}(P_1) \cdot ... \cdot f_{P_N}(P_N) \cdot c(F_{P_i}(P_i),...,F_{P_N}(P_N))$, where F_{P_i} is the cumulative distribution function (CDF) of P_i. Therefore, from a statistical perspective, the changes in the spatial scale extremes, which are associated with changes in $f(P_1, ..., P_N)$, can be decomposed into changes in (1) the magnitude of the precipitation extremes (i.e., the marginal distributions) and (2) the spatial dependence between precipitation at neighboring locations (i.e., the copula) (Bevacqua, Vousdoukas, et al., 2020).

We estimate (1) as $100 \times (SS_{magn} - SS_{pres})/SS_{pres}$, where SS_{pres} is the spatial scale extreme in the present and SS_{magn} is the spatial scale extreme in a data set that assumes changes in precipitation magnitude, but not in spatial dependence (pairwise Spearman's correlations and tail dependencies [Bevacqua et al., 2017]). Following Bevacqua et al. (2019) (and, e.g., Manning et al., 2019; Villalobos-Herrera et al., 2020), this data set is defined as $F_{P_{fut1}}^{-1}(F_{P_{pres1}}(P_{pres1})),...,F_{P_{futN}}^{-1}(F_{P_{presN}}(P_{presN}))$, where $P_{pres\,i}$ and $F_{P_{pres\,i}}$ are the wintertime precipitation in the present and its empirical CDF, respectively; and $P_{fut\,i}$ and $F_{P_{fut\,i}}$ are the same, but for the future. Given that $F_{P_{pres\,i}}(P_{pres\,i})$ has a standard uniform distribution, the marginal pdfs of the variables in

Present-day precipitation spatial scale extremes
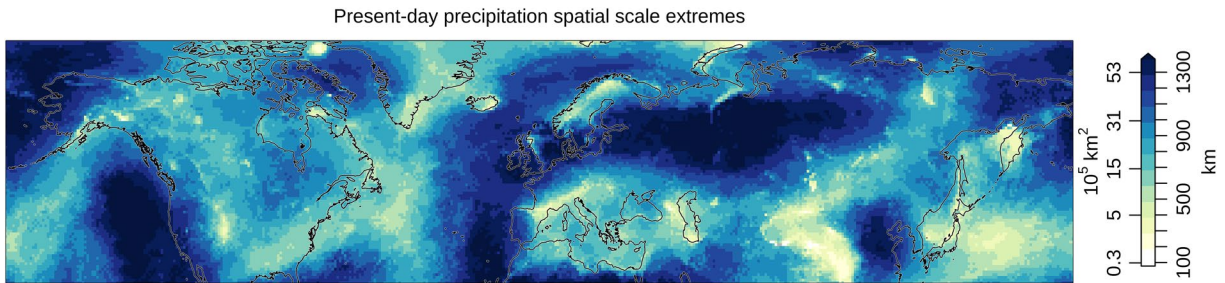
Figure 1. Present-day spatial scale extreme, defined as the 100-year return level of the wintertime precipitation extremes' spatial scale ($T_{occur} = 10$ years; Methods). The colors indicate both the spatial scale value SS (i.e., a circular area in km^2) and the associated radius in km, that is, $\sqrt{SS / \pi}$.

the data set are as in the future; the copula is a function of the variables $(F_{P_{pres\,1}}(P_{pres\,1}),\ldots,F_{P_{pres\,N}}(P_{pres\,N}))$ and is, therefore, as in the present.

Similarly, we estimate (2) as $100 \times (SS_{dep} - SS_{pres})/SS_{pres}$, where SS_{dep} is the spatial scale's extreme in the data set $(F_{P_{pres1}}^{-1}(F_{P_{fut1}}(P_{fut\,1}))),\ldots,(F_{P_{presN}}^{-1}(F_{P_{futN}}(P_{fut\,N})))$, which assumes changes in precipitation spatial dependence (copula as in the future), but not in precipitation magnitudes.

2.5. Area Weighted Aggregated Statistics

All the statistics, such as median, pattern Spearman's correlations ($\rho_{Spearman}^{pattern}$), and percentage of the analyzed area, are weighted based on the grid-points' surfaces, using the R-packages *wCorr* (Emad & Bailey, 2017) and *spatstat* (Baddeley et al., 2004).

3. Results

3.1. Present-Day Spatial Scale Extremes

Given that simultaneous extremely wet winters occurring at multiple locations within the same region can enhance regional impacts, we analyze the extreme extents of these events employing the precipitation spatial scale. The present-day spatial scale extremes are shown in Figure 1. A small spatial scale extreme indicates that precipitation extremes tend to be localized, that is, to not co-occur with extremes in the surrounding area. The hemispheric median of the spatial scale extremes is about 28×10^5 km^2 (i.e., a circular area associated with a radius of 940 km), indicating that the considered events potentially extend across multiple countries. Note that, as local precipitation extreme magnitudes are defined based on local return levels, small and large extents are associated with small and large regional spatial dependencies in the precipitation field, respectively.

Across the Northern Hemisphere extratropics, there is large variability in the spatial scale extremes, hence in the spatial dependencies, of the precipitation field (Figure 1), which appears to be influenced by topography. In fact, there is a tendency toward larger and smaller spatial scale extremes at lower and higher altitudes, respectively (Figure S2), which is in line with the results found by Berghuijs et al. (2019) for European river flooding spatial scales. The largest spatial scale extremes occur over northern Europe, Russian plains, eastern China, and oceans; that is, typically over extended low altitude areas, where the occurrence of widespread precipitation extremes is not obstructed by the orography. For example, in Moscow (Russia), the most extended events are associated with an anomalous seasonal upper-level atmospheric jet over central Europe (Figure S3) and associated cyclonic activity, which—given the flat topography—favors widespread precipitation extremes in the surrounding area (Harvey et al., 2020; Hawcroft et al., 2012). The mean altitude of the locations with the top 5% (1%) spatial scale extremes is 130 m (80 m), against an average altitude of 370 m over the analyzed area. In contrast, the lowest spatial scales are typically found across mountainous areas, where precipitation extremes can be localized due to orographic effects (Martius et al., 2016), such as the Rocky Mountains, Alps and Pyrenees, Scandinavian Mountains, Caucasus Mountains, Himala-

yas, and Gobi Desert. As a result, the mean altitude of the locations with the 5% (1%) smallest spatial scale extremes is 980 m (2000 m).

A comparison of the results based on the HadAM4 model and the ERA5 reanalysis is not possible for very extreme events due to the limited sample size of the reanalysis data (e.g., van den Hurk et al., 2015; van der Wiel et al., 2019). This is the case even when considering ERA5 data during the extended period 1980–2020, therefore we focus the evaluation on less extreme events. The biases in the wintertime mean and 5-year return level precipitation are in line with those of other global climate models (Figures S4 and S5), with a good representation of broad-scale features (Flato et al., 2014; Watson et al., 2020). Even for the considered relatively low return levels (T_{occur} = 5 years, T_{SS} = 10 years), the spatial pattern of the spatial scale high values in ERA5 is spatially noisy compared to HadAM4 (Figure S6), highlighting that large ensemble simulations are essential for analyzing spatially extended wintertime precipitation extremes and that an evaluation of these events is challenging. Nevertheless, the similarity of the area-weighted spatial scale (median of the associated radius of 540 and 440 km in HadAM4 and ERA5, respectively) and of the large-scale spatial pattern indicates that the HadAM4 model performs well for the purpose of the study.

3.2. Projected Changes in the Spatial Scale Extremes and Associated Drivers

In a world 2.0 °C warmer than during pre-industrial conditions, the extent of precipitation extremes is projected to increase over 90% of the analyzed area (Figure 2a; Figure S7a shows changes in km^2). Spatial scale extremes increase by 93% in median (note that the increase is higher on landmasses than over ocean). Notably, such an increase corresponds to a median growth of 29×10^5 km^2 in spatial scale, which is equal to more than 10 times the surface area of a country such as the United Kingdom. Over 20% of the analyzed area, the spatial scale increases by at least 240% (71×10^5 km^2).

At the regional scale, the strongest percentage increase occurs over Canada, that is, 390% (96×10^5 km^2; median over the box in Figure S7a). Over Northern Europe, a large increase in the spatial scale (71×10^5 km^2; Figure S7a) combined with the relatively small present-day spatial-scale around the Scandinavian Mountains (Figure 1) results in a substantial, that is, by 190%, percentage increase in the extents. The increase is particularly large also over central and eastern Asia (250%; 60×10^5 km^2); however, note that the regional wintertime precipitation is frequently lower than about 0.2 mm/day (i.e., about 18 mm/season; gray contours in Figure 2d), hence changes in the extents may have small impacts in this region. Overall, land areas with a substantial reduction in the extents are limited to Northern Africa, Spain and Portugal (−24%; $−8.3 \times 10^5$ km^2). The strongest reduction in the extents is projected over the Labrador Sea.

Most of the projected extent changes are incompatible with variations due to interannual variability (see stippling in Figure 2a), highlighting the presence of clear global warming induced effects. We move on to understanding the sources of these trends through decomposing the extent changes into the contributions from changes in the spatial dependence and magnitudes of the precipitation field.

3.2.1. Drivers of the Changes in the Spatial Scale Extremes

Changes in the spatial dependence of the precipitation field lead to generally small changes in the extent of the events (Figure 2b; median of about −1%). Such dependence-related changes are rarely statistically significant and do not exhibit a clear large-scale spatial pattern. The above indicates that the change in the spatial organization of the wintertime precipitation extreme occurrences is generally unimportant for changes in the extreme spatial extents. Consistently, the changes in the spatial scales are dominated by the other potential driver, that is, changes in the precipitation magnitude (compare Figures 2a and 2c; $\rho_{Spearman}^{pattern}$ = 0.93). In fact, similarly to the actual changes in the spatial scale (Figure 2a), changes in the spatial scale resulting from precipitation magnitude changes (Figure 2c) are large, that is, 91% in median, and positive over 92% of the analyzed area. In line with this, the spatial pattern of the change in the precipitation extent resembles that of the change in the precipitation magnitudes (Figures 2a and 2d; $\rho_{Spearman}^{pattern}$ = 0.74). Remarkably, relatively small regional percentage changes in precipitation magnitude can result in a large percentage
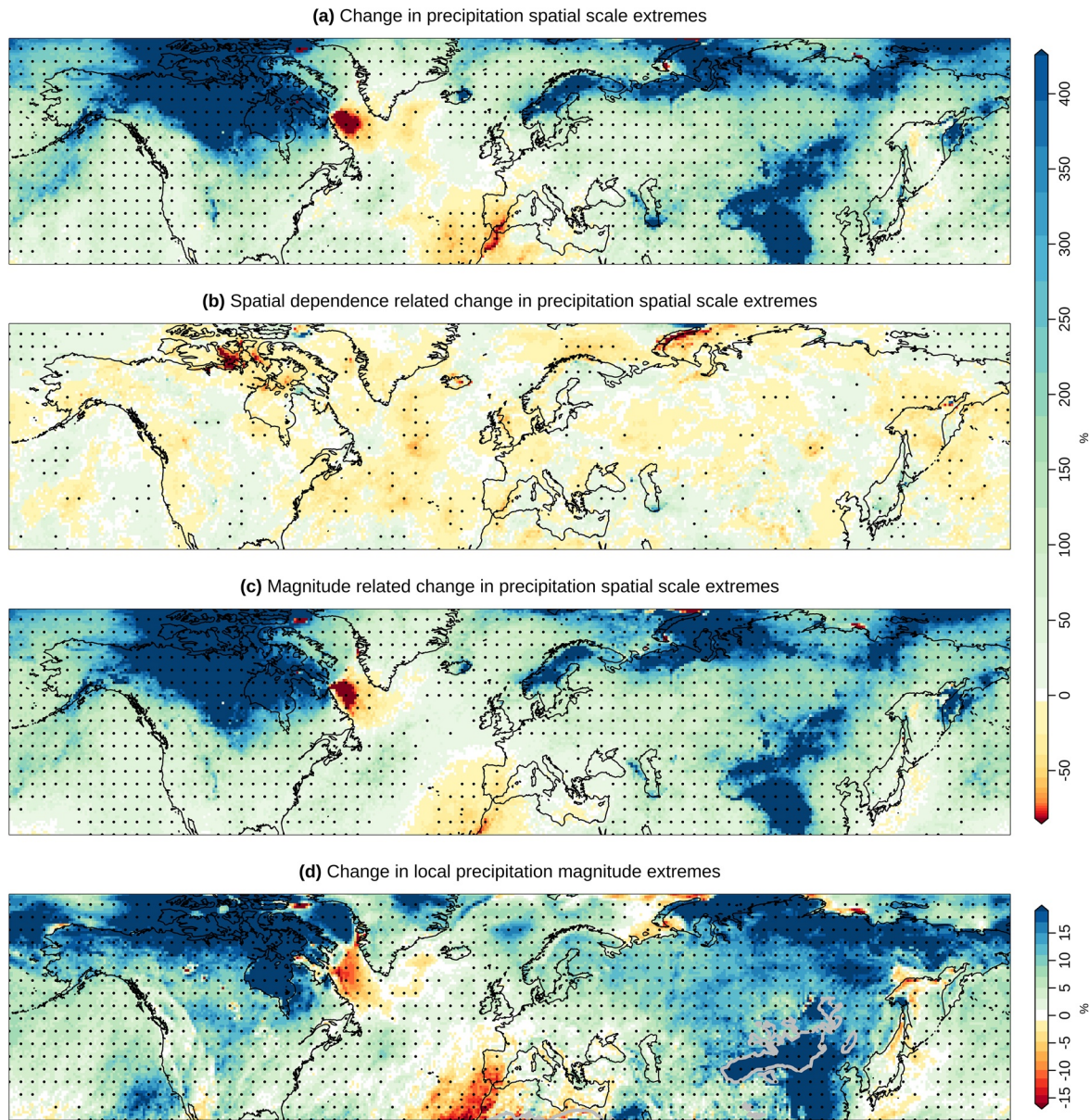
Figure 2. (a) Change in the spatial scale extreme in a 2.0 °C warming scenario. The spatial scale extreme is defined as the 100-year return level of the wintertime precipitation extremes' spatial scale (T_{occur} = 10 years; Methods). Change in the spatial scale extremes caused by changes in (b) spatial dependencies in the precipitation field and (c) precipitation magnitudes. Stippling indicates statistically significant changes (Methods). (d) Change in the 10-year return level of the local wintertime precipitation total; gray contours over Asia enclose areas where the present-day 10-year return level is below 0.2 mm/day (i.e., about 18 mm/season). The color palette is chosen such that inverse changes between future and present values have the same color intensity, for example, −50% (halving) and +100% (doubling) are shown with the same color intensity.

change in the spatial extent of the extremes (Figures 2a and 2d). In fact, the median percentage increase in the spatial scale extremes (93%) is about 23 times larger than the increase in the magnitudes (about 4%).

From a physical perspective, all the above implies that the changes in the spatial extent can be understood in terms of the physical processes that modulate the changes in the precipitation extreme magnitudes. At the large scale, in line with other studies, precipitation magnitudes are projected to widely increase in percentage over the Northern Hemisphere extratropics landmasses, especially at high latitudes and over Asia, and to decrease around Northern Africa and northwestern Mexico (Figure 2d; Figure S7b shows changes in mm/day) (e.g., Knutti & Sedláček, 2013; Scoccimarro & Gualdi, 2020; Zappa et al., 2021). The widespread increase in precipitation magnitudes arises from thermodynamic effects, that is, in a warmer world,

a higher atmospheric moisture holding capacity leads to more intense precipitation (e.g., Pfahl et al., 2017). However, atmospheric circulation changes, in which we have less confidence (Shepherd, 2014), will also substantially modulate regional precipitation changes and can either compensate or enhance the thermo-dynamic effect (Bevacqua, Zappa, et al., 2020; Pfahl et al., 2017). To illustrate the different effects that documented atmospheric circulation changes can have on the magnitude, and therefore extent, of precipitation extremes, we now consider three case studies, focused on locations characterized by strong climate change effects. The similarity of the projected atmospheric circulation changes with those documented by previous research highlights the plausibility of the precipitation changes presented in our study.

3.2.2. Case Studies

To begin with, the strong reduction in precipitation magnitudes over northern Africa (about −10% in Marrakesh; Morocco)—which contributes to the reduced extents of the spatial scale extremes in the surrounding region—is in line with documented changes in the atmospheric circulation that would reduce both daily precipitation extremes (Pfahl et al., 2017) and total wintertime precipitation (Zappa & Shepherd, 2017). In fact, in Marrakesh, sustained upper-level winds over northern Africa, which are associated with stormy weather (Harvey et al., 2020; Zappa, Hoskins, et al., 2015), favor high precipitation amounts around the city, northwestern Africa, and the central and western Mediterranean region (Figure 3a). In a warmer climate, this atmospheric circulation feature is expected to significantly weaken both during extremely wet winters and on average (Figure 3c; compare with Figure 3a), which is in line with a documented weakening and reduction of storm intensity and frequency (Bevacqua, Zappa, et al., 2020; Harvey et al., 2020; Pinto et al., 2007; Zappa, Hawcroft, et al., 2015). As a result, precipitation extreme magnitudes and extents would decrease (Figure 3b; see also the reduced stippling around Marrakesh compared to Figure 3a), despite a higher atmospheric moisture content (Li et al., 2018; Pfahl et al., 2017).

Over the Scandinavian Peninsula, where extents are projected to increase strongly, precipitation magnitudes are projected to increase substantially, that is, by about 10%, which is more than twice the hemispheric median increase. Wintertime precipitation extremes in this region are typically driven by an anomalously strong jet stream configuration over the United Kingdom (Figure 3d) and associated storminess. Under a 2.0 °C warming scenario, a significant strengthening of such a configuration (Figure 3f; compare with Figure 3d) would, therefore, favor the substantial increase in precipitation extremes and associated spatial extents (Figure 3e; see also more frequent stippling compared to Figure 3d) (Harvey et al., 2020; Li et al., 2018; Zappa et al., 2013). We observe that given that precipitation over the Scandinavian Peninsula is mainly driven by cyclones (Hawcroft et al., 2012; Pfahl & Wernli, 2012) and a sustained jet stream is associated with an increased cyclone activity, such an atmospheric circulation change would be consistent with a strengthening of the regional cyclonic activity (Harvey et al., 2020; Pinto et al., 2007; Zappa et al., 2013).

Finally, we consider the case of Wuhan (China), characterized by the highest projected increase in accumulated precipitation; the 10-year return level increases by more than 20% (about 1 mm/day, i.e., 90 mm/season). Around the Chinese city, precipitation extremes are associated with an atmospheric circulation pattern characterized by weakened upper-level westerly winds across Japan and southern China (Figure 3g), in line with a weak East Asian winter monsoon (EAWM; L. Wang & Chen, 2014). The future strong intensification of precipitation (Figure 3h) is therefore consistent with a general enhancement of such an atmospheric circulation pattern (Figure 3i; compare with Figure 3g). Note that this projected wintertime evolution of the jet stream represents a plausible storyline of future atmospheric circulation change according to other climate model projections (Harvey et al., 2020; Li et al., 2018; Pinto et al., 2007), and appears in line with a projected weakening of the EAWM (Kitoh, 2006; H. Wang et al., 2013).

3.3. Difference Between Changes Under 1.5 °C and 2.0 °C Warming Scenarios

Understanding how 0.5 °C less warming relative to +2.0 °C can reduce climate-related impacts is key for climate policies (Mitchell et al., 2016); gaining such an understanding requires large-ensemble simulations (Mitchell, AchutaRao, et al., 2017; Uhe et al., 2021). The general spatial pattern of the changes under 2.0 °C and 1.5 °C warming scenarios is similar ($\rho_{\text{Spearman}}^{pattern} = 0.87$, increasing spatial scale extremes over 90% and 87% of the area, respectively; Figure 2a and Figure S8a). However, the median increase in the spatial scale
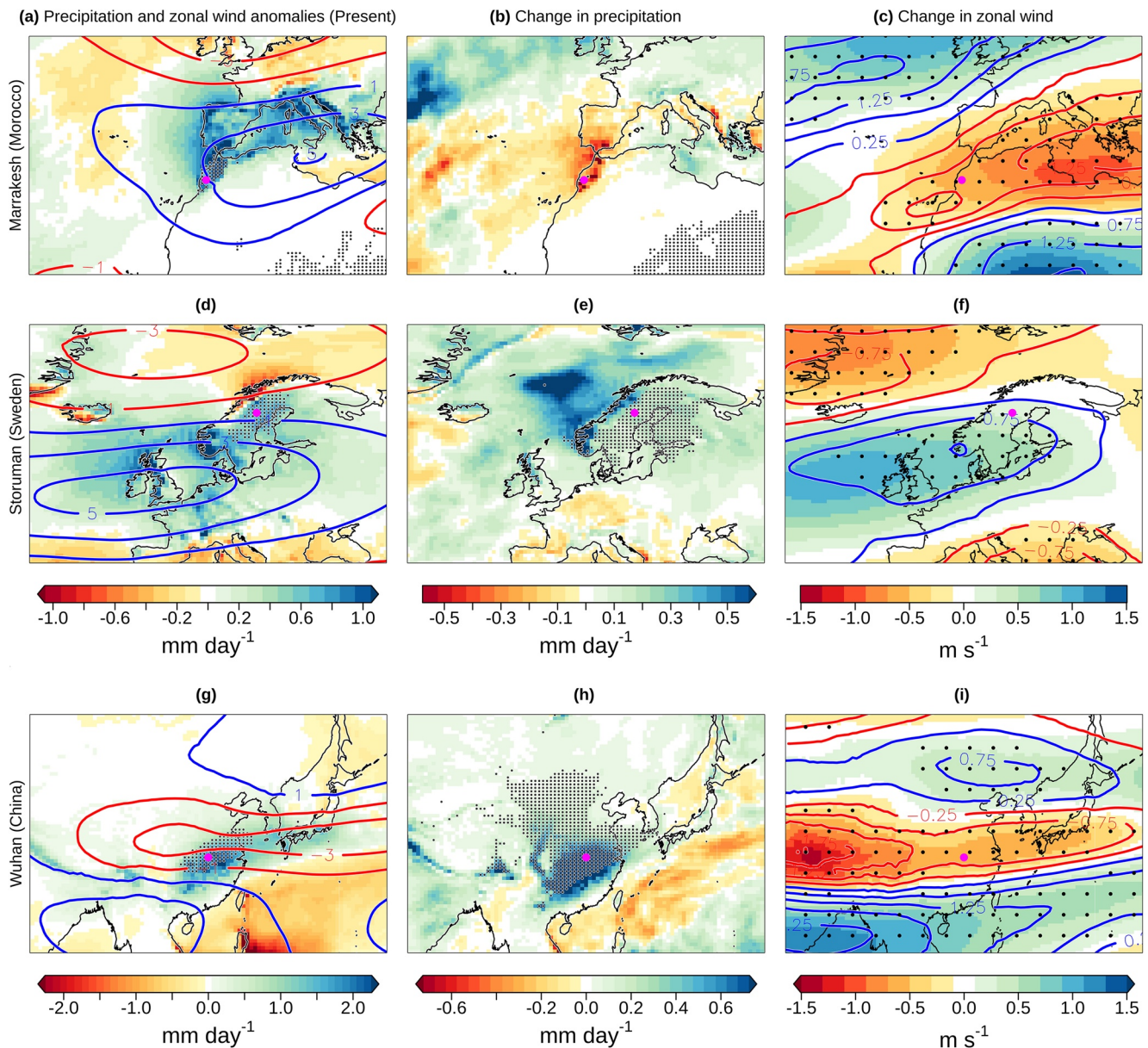
Figure 3. (a) Average of the present-day anomaly in the wintertime total precipitation (shading) and zonal wind at 250 hPa (contours; blue/red for positive/ negative values) fields during extremely wet winters in Marrakesh (Morocco; shown with a magenta dot). (b) Projected change in the mean of the precipitation during extremely wet winters in Marrakesh under a +2.0 °C warming scenario. In the present (future), extremely wet winters are defined as those where the precipitation in Marrakesh is above the present (future) 10-year return level. In (a)/(b), stippling indicates locations where the average precipitation in the present/future is higher than the present-day 10-year return level. (c) Change in the average of the zonal wind at 250 hPa during extremely wet winters (contours) and during all winters (shading). Black stippling indicates significant changes of the wind during extremely wet winters (i.e., future wind lying outside the present-day centered 95% confidence interval (CI); the CI is estimated through re-sampling present-day extreme events). Panels (d–f) and (g–i) are as in (a–c), but for Storuman (Sweden) and Wuhan (China), respectively.

extremes would be about 1.7 times higher in a 2.0 °C (93%) than in a 1.5 °C warming scenario (55%). Such a difference is qualitatively in line with the changes in precipitation magnitude, which increases by about 4% and 3% in median under 2.0 °C and 1.5 °C warming scenarios, respectively (Figure 2d and Figure S8b). Stabilizing global warming at 2 °C rather than 1.5 °C would at least double the increase in the spatial scale extremes over 35% of the area that shows larger extents in both scenarios, and at least quadruple it over 9% of the area.

Parts of Spain and Portugal are the noticeable landmasses where the spatial scale extremes would increase in a 1.5 °C warming scenario, but reverse, that is, decrease, in a 2.0 °C warming scenario (Figure S8a and Figure 2a). Such a reversal is in line with the changes in precipitation intensities which would increase to a certain extent in a 1.5 °C scenario but decrease in a 2.0 °C scenario (Figure S8b and Figure 2d). This is consistent with a strong weakening of the upper-level winds over northern Africa across the two scenarios (Figure S9), which would reverse the thermodynamically driven precipitation increase (Li et al., 2018).

4. Discussion and Conclusions

The spatial extent of the wintertime total precipitation extremes is projected to increase notably across most of the Northern Hemisphere extratropics in a 1.5 °C and 2.0 °C warming scenario. Such growth in spatial extent is largely driven by increased wintertime precipitation extreme magnitudes. Given that extended high wintertime precipitation totals are driven by multiple weather systems moving across the same region (Hawcroft et al., 2012; Zappa, Hawcroft, et al., 2015), our projection is consistent with the documented increase in the precipitation accumulated around the tracks of individual weather systems (Bevacqua, Zappa, et al., 2020; Prein et al., 2017).

Our large-scale projection of precipitation extreme magnitudes, which is the main driver of the extent growth, is in line with projections from other modeling and experimental designs, including inter-comparisons, for example, CMIP (Knutti & Sedláček, 2013; Pfahl et al., 2017; Uhe et al., 2021). Regionally, that is, around the Mediterranean basin and Mexico, the direction of the future changes is more uncertain across models (Bevacqua, Zappa, et al., 2020; Pfahl et al., 2017; Shepherd, 2014; Uhe et al., 2021). In fact, regional precipitation extent changes can depend on the model-dependent storyline of atmospheric circulation response to climate change (Bevacqua, Zappa, et al., 2020; Zappa & Shepherd, 2017). At a specific level of global warming, uncertainty in the atmospheric circulation and precipitation response can also arise from differences in the definition of the forcing (GHG relative to aerosol) leading to the given warming level (Uhe et al., 2021). Therefore, users interested in regional-scale changes in precipitation spatial extents should interpret our projection as a specific plausible storyline. For example, a weaker reduction of the upper-level winds over northern Africa than that found here is also plausible and could lead to a weaker decrease in the magnitude and spatial scales of precipitation extremes around southern Europe (Bevacqua, Zappa, et al., 2020; Li et al., 2018; Zappa, 2019; Zappa, Hoskins, et al., 2015). We find that changes in the spatial organization, that is, dependencies, of the precipitation extremes only marginally affect the future extent changes. This is consistent with the unchanged topography that would constrain potential changes in the spatial dependencies. However, given that atmospheric circulation changes may also modulate dependency changes, we cannot exclude the plausibility of an alternative storyline characterized by changes in the spatial dependencies.

Further studies based on large ensemble simulations from alternative climate model setups (including regional climate models, which can improve the representation of local extremes) will allow for a comprehensive assessment of the regional precipitation extent changes. Our results indicate that an important contribution from intensified precipitation toward a growth in the extents is likely a general feature of climate models in areas of the world where higher wintertime precipitation extremes are projected. Notably, to assume that percentage changes in precipitation intensities will drive similar percentage changes in the extent would be highly misleading. In fact, relatively small percentage increases in precipitation intensities can drive disproportionately larger, by 1–2 orders of magnitude (Table S2 shows the sensitivity to the return periods), increases in the extent of the events. The estimated spatial extent increase depends on the degree of extremeness of the considered events (Table S1).

Precipitation is a relevant driver of spatially extended flooding (Jongman et al., 2014), hence the growth in the precipitation extreme extents could substantially impact areas across the Northern Hemisphere extratropics. Stabilizing global warming at 1.5 °C rather than 2.0 °C, in line with the Paris Agreement, may substantially reduce impacts. Our study can contribute to understanding flooding changes, which also depend on, for example, soil moisture, snowmelt, exposure, and vulnerability dynamics (Brunner et al., 2020; Jongman et al., 2014; Kemter et al., 2020). Overall, neglecting the spatial footprint of precipitation extreme events could lead to underestimating the population that is simultaneously affected by hazardous

conditions. Hence, considering the effect of simultaneous extremes across neighboring countries could allow for developing a better international preparedness for extreme events.

Conflict of Interest

The authors declare no competing interests.

Data Availability Statement

The data used in this study are available through Bevacqua, Watson, et al. (2020) at http://doi.org/10.5281/zenodo.4311221. ERA5 reanalysis is available through Hersbach et al. (2020) at https://climate.copernicus.eu/climate-reanalysis.

References

Baddeley, A. J., & Turner, R. (2004). *Spatstat: An R package for analyzing spatial point pattens.* Department of Mathematics and Statistics, University of Western Australia.

Berghuijs, W. R., Allen, S. T., Harrigan, S., & Kirchner, J. W. (2019). Growing spatial scales of synchronous river flooding in Europe. *Geophysical Research Letters*, *46*(3), 1423–1428. https://doi.org/10.1029/2018gl081883

Bevacqua, E., Maraun, D., Hobæk Haff, I., Widmann, M., & Vrac, M. (2017). Multivariate statistical modelling of compound events via pair-copula constructions: Analysis of floods in Ravenna (Italy). *Hydrology and Earth System Sciences*, *21*(6), 2701–2723. https://doi.org/10.5194/hess-21-2701-2017

Bevacqua, E., Maraun, D., Vousdoukas, M. I., Voukouvalas, E., Vrac, M., Mentaschi, L., & Widmann, M. (2019). Higher probability of compound flooding from precipitation and storm surge in Europe under anthropogenic climate change. *Science Advances*, *5*(9), eaaw5531. https://doi.org/10.1126/sciadv.aaw5531

Bevacqua, E., Vousdoukas, M. I., Zappa, G., Hodges, K., Shepherd, T. G., Maraun, D., et al. (2020). More meteorological events that drive compound coastal flooding are projected under climate change. *Communications Earth & Environment*, *1*(47). https://doi.org/10.1038/s43247-020-00044-z

Bevacqua, E., Watson, P., Sparrow, S., & Wallom, D. (2020). *Multi-thousand-year simulations of December-February precipitation and zonal upper-level wind (Version 1.0.0) [Data set]*. Zenodo. http://doi.org/10.5281/zenodo.4311221

Bevacqua, E., Zappa, G., & Shepherd, T. G. (2020). Shorter cyclone clusters modulate changes in European wintertime precipitation extremes. *Environmental Research Letters*, *15*, 124005. https://doi.org/10.1088/1748-9326/abbde7

Brunner, M. I., Gilleland, E., Wood, A., Swain, D. L., & Clark, M. (2020). Spatial dependence of floods shaped by spatiotemporal variations in meteorological and land-surface processes. *Geophysical Research Letters*, *47*(13), e2020GL088000. https://doi.org/10.1029/2020gl088000

Chang, W., Stein, M. L., Wang, J., Kotamarthi, V. R., & Moyer, E. J. (2016). Changes in spatiotemporal precipitation patterns in changing climate conditions. *Journal of Climate*, *29*(23), 8355–8376. https://doi.org/10.1175/jcli-d-15-0844.1

Demory, M.-E., Vidale, P. L., Roberts, M. J., Berrisford, P., Strachan, J., Schiemann, R., & Mizielinski, M. S. (2014). The role of horizontal resolution in simulating drivers of the global hydrological cycle. *Climate Dynamics*, *42*(7–8), 2201–2225. https://doi.org/10.1007/s00382-013-1924-4

Dwyer, J. G., & O'Gorman, P. A. (2017). Changing duration and spatial extent of midlatitude precipitation extremes across different climates. *Geophysical Research Letters*, *44*(11), 5863–5871. https://doi.org/10.1002/2017gl072855

Emad, A., & Bailey, P. (2017). *wcorr: Weighted correlations—R package version 1.9.1.*

Enríquez, A. R., Wahl, T., Marcos, M., & Haigh, I. D. (2020). Spatial footprints of storm surges along the global coastlines. *Journal of Geophysical Research: Oceans*, *125*(9), e2020JC016367. https://doi.org/10.1029/2020jc016367

Flato, G., Marotzke, J., Abiodun, B., Braconnot, P., Chou, S. C., Collins, W., et al. (2014). Evaluation of climate models. In T. F. Stocker, D. Qin, G.-K. Plattner, M. Tignor, S. K. Allen, J. Doschung, et al. (Eds.), *Climate change 2013: The physical science basis. Contribution of working group I to the fifth assessment report of the intergovernmental panel on climate change* (pp. 741–866). Cambridge University Press.

Guinard, K., Mailhot, A., & Caya, D. (2015). Projected changes in characteristics of precipitation spatial structures over North America. *International Journal of Climatology*, *35*(4), 596–612. https://doi.org/10.1002/joc.4006

Harvey, B., Cook, P., Shaffrey, L., & Schiemann, R. (2020). The response of the northern hemisphere storm tracks and jet streams to climate change in the CMIP3, CMIP5, and CMIP6 climate models. *Journal of Geophysical Research: Atmospheres*, *125*, e2020JD032701. https://doi.org/10.1029/2020JD032701

Hawcroft, M., Shaffrey, L., Hodges, K., & Dacre, H. (2012). How much northern hemisphere precipitation is associated with extratropical cyclones? *Geophysical Research Letters*, *39*(24). https://doi.org/10.1029/2012gl053866

Hersbach, H., Bell, B., Berrisford, P., Hirahara, S., Horányi, A., Muñoz-Sabater, J., et al. (2020). The ERA5 global reanalysis. *Quarterly Journal of the Royal Meteorological Society*, *146*(730), 1999–2049. https://doi.org/10.1002/qj.3803

Hoegh-Guldberg, O., Jacob, D., Bindi, M., Brown, S., Camilloni, I., Diedhiou, A., et al. (2018). *Impacts of 1.5ºC global warming on natural and human systems*. Global warming of 1.5ºC: An IPCC Special Report.

Jongman, B., Hochrainer-Stigler, S., Feyen, L., Aerts, J. C. J. H., Mechler, R., Botzen, W. J. W., et al. (2014). Increasing stress on disaster-risk finance due to large floods. *Nature Climate Change*, *4*(4), 264–268. https://doi.org/10.1038/nclimate2124

Kemter, M., Merz, B., Marwan, N., Vorogushyn, S., & Blöschl, G. (2020). Joint trends in flood magnitudes and spatial extents across Europe. *Geophysical Research Letters*, *47*(7), e2020GL087464. https://doi.org/10.1029/2020gl087464

Kendon, M., & McCarthy, M. (2015). The UK's wet and stormy winter of 2013/2014. *Weather*, *70*(2), 40–47. https://doi.org/10.1002/wea.2465

Kitoh, A. (2006). Asian monsoons in the future. In B. Wang (Ed.), *The asian monsoon* (pp. 631–649). Springer.

Knutti, R., & Sedláček, J. (2013). Robustness and uncertainties in the new CMIP5 climate model projections. *Nature Climate Change*, *3*(4), 369–373. https://doi.org/10.1038/nclimate1716

Leonard, M., Westra, S., Phatak, A., Lambert, M., van den Hurk, B., McInnes, K., et al. (2014). A compound event framework for understanding extreme impacts. *WIREs Climate Change*, *5*(1), 113–128. https://doi.org/10.1002/wcc.252

Li, C., Michel, C., Seland Graff, L., Bethke, I., Zappa, G., Bracegirdle, T. J., et al. (2018). Midlatitude atmospheric circulation responses under 1.5 and 2.0°C warming and implications for regional impacts. *Earth System Dynamics*, *9*(2), 359–382. https://doi.org/10.5194/esd-9-359-2018

Manning, C., Widmann, M., Bevacqua, E., Van Loon, A. F., Maraun, D., & Vrac, M. (2019). Increased probability of compound long-duration dry and hot events in Europe during summer (1950–2013). *Environmental Research Letters*, *14*(9), 094006. https://doi.org/10.1088/1748-9326/ab23bf

Martius, O., Pfahl, S., & Chevalier, C. (2016). A global quantification of compound precipitation and wind extremes. *Geophysical Research Letters*, *43*(14), 7709–7717. https://doi.org/10.1002/2016gl070017

Mitchell, D., AchutaRao, K., Bethke, I., Beyerle, U., Ciavarella, A., Forster, P., et al. (2017). Half a degree additional warming, prognosis and projected impacts (HAPPI): Background and experimental design. *Geoscientific Model Development*, *10*, 571–583.

Mitchell, D., Davini, P., Harvey, B., Massey, N., Haustein, K., Woollings, T., et al. (2017). Assessing mid-latitude dynamics in extreme event attribution systems. *Climate Dynamics*, *48*(11–12), 3889–3901. https://doi.org/10.1007/s00382-016-3308-z

Mitchell, D., James, R., Forster, P. M., Betts, R. A., Shiogama, H., & Allen, M. (2016). Realizing the impacts of a 1.5°C warmer world. *Nature Climate Change*, *6*(8), 735–737. https://doi.org/10.1038/nclimate3055

Nikumbh, A. C., Chakraborty, A., & Bhat, G. (2019). Recent spatial aggregation tendency of rainfall extremes over India. *Scientific Reports*, *9*(1), 1–7. https://doi.org/10.1038/s41598-019-46719-2

O'Gorman, P. A., & Schneider, T. (2009). The physical basis for increases in precipitation extremes in simulations of 21st-century climate change. *Proceedings of the National Academy of Sciences of the United States of America*, *106*(35), 14773–14777.

Pfahl, S., O'Gorman, P. A., & Fischer, E. M. (2017). Understanding the regional pattern of projected future changes in extreme precipitation. *Nature Climate Change*, *7*(6), 423–427. https://doi.org/10.1038/nclimate3287

Pfahl, S., & Wernli, H. (2012). Quantifying the relevance of cyclones for precipitation extremes. *Journal of Climate*, *25*(19), 6770–6780. https://doi.org/10.1175/jcli-d-11-00705.1

Pinto, J. G., Ulbrich, U., Leckebusch, G., Spangehl, T., Reyers, M., & Zacharias, S. (2007). Changes in storm track and cyclone activity in three SRES ensemble experiments with the ECHAM5/MPI-OM1 GCM. *Climate Dynamics*, *29*(2–3), 195–210. https://doi.org/10.1007/s00382-007-0230-4

Prein, A. F., Liu, C., Ikeda, K., Trier, S. B., Rasmussen, R. M., Holland, G. J., & Clark, M. P. (2017). Increased rainfall volume from future convective storms in the US. *Nature Climate Change*, *7*(12), 880–884. https://doi.org/10.1038/s41558-017-0007-7

Schaller, N., Kay, A. L., Lamb, R., Massey, N. R., Van Oldenborgh, G. J., Otto, F. E. L., et al. (2016). Human influence on climate in the 2014 southern England winter floods and their impacts. *Nature Climate Change*, *6*(6), 627–634. https://doi.org/10.1038/nclimate2927

Scoccimarro, E., & Gualdi, S. (2020). Heavy daily precipitation events in the CMIP6 worst-case scenario: Projected twenty-first-century changes. *Journal of Climate*, *33*(17), 7631–7642. https://doi.org/10.1175/jcli-d-19-0940.1

Shepherd, T. G. (2014). Atmospheric circulation as a source of uncertainty in climate change projections. *Nature Geoscience*, *7*(10), 703–708. https://doi.org/10.1038/ngeo2253

Sklar, M. (1959). Fonctions de repartition an dimensions et leurs marges (*8*, pp. 229–231). Publications de I'Institut de Statistique de l'University de Paris.

Touma, D., Michalak, A. M., Swain, D. L., & Diffenbaugh, N. S. (2018). Characterizing the spatial scales of extreme daily precipitation in the United States. *Journal of Climate*, *31*(19), 8023–8037. https://doi.org/10.1175/jcli-d-18-0019.1

Trzeciak, T. M., Knippertz, P., Pirret, J. S., & Williams, K. D. (2016). Can we trust climate models to realistically represent severe European windstorms? *Climate Dynamics*, *46*(11–12), 3431–3451. https://doi.org/10.1007/s00382-015-2777-9

Uhe, P., Mitchell, D., Bates, P. D., Allen, M. R., Betts, R. A., Huntingford, C., et al. (2021). Method uncertainty is essential for reliable confidence statements of precipitation projections. *Journal of Climate*, *34*, 1227–1240. https://doi.org/10.1175/JCLI-D-20-0289.1

van derHurk, B., van Meijgaard, E., de Valk, P., van Heeringen, K.-J., & Gooijer, J. (2015). Analysis of a compounding surge and precipitation event in The Netherlands. *Environmental Research Letters*, *10*(3), 035001. https://doi.org/10.1088/1748-9326/10/3/035001

van der Wiel, K., Stoop, L. P., Van Zuijlen, B., Blackport, R., Van den Broek, M., & Selten, F. (2019). Meteorological conditions leading to extreme low variable renewable energy production and extreme high energy shortfall. *Renewable and Sustainable Energy Reviews*, *111*, 261–275.

Villalobos-Herrera, R., Bevacqua, E., Ribeiro, A. F., Auld, G., Crocetti, L., Mircheva, B., et al. (2020). Towards a compound event-oriented climate model evaluation: A decomposition of the underlying biases in multivariate fire and heat stress hazards. *Natural Hazards and Earth System Sciences Discussions*. https://doi.org/10.5194/nhess-2020-383

Wang, H., He, S., & Liu, J. (2013). Present and future relationship between the East Asian winter monsoon and ENSO: Results of CMIP5. *Journal of Geophysical Research: Oceans*, *118*(10), 5222–5237. https://doi.org/10.1002/jgrc.20332

Wang, L., & Chen, W. (2014). An intensity index for the East Asian winter monsoon. *Journal of Climate*, *27*(6), 2361–2374. https://doi.org/10.1175/jcli-d-13-00086.1

Wasko, C., Sharma, A., & Westra, S. (2016). Reduced spatial extent of extreme storms at higher temperatures. *Geophysical Research Letters*, *43*(8), 4026–4032. https://doi.org/10.1002/2016gl068509

Watson, P., Sparrow, S., Ingram, W., Wilson, S., Marie, D., Zappa, G., et al. (2020). *Multi-thousand member ensemble atmospheric simulations with global 60 km resolution using climateprediction.net* (p. 10895). Paper preseneted at EGU General Assembly Conference Abstracts. https://doi.org/10.5194/egusphere-egu2020-10895

Williams, K., Ringer, M., & Senior, C. (2003). Evaluating the cloud response to climate change and current climate variability. *Climate Dynamics*, *20*(7–8), 705–721. https://doi.org/10.1007/s00382-002-0303-3

Zappa, G. (2019). Regional climate impacts of future changes in the mid-latitude atmospheric circulation: A storyline view. *Current Climate Change Reports*, *5*(4), 358–371. https://doi.org/10.1007/s40641-019-00146-7

Zappa, G., Bevacqua, E., & Shepherd, T. G. (2021). Communicating potentially large but non-robust changes in multi-model projections of future climate. *International Journal of Climatology*. https://doi.org/10.1002/joc.7041

Zappa, G., Hawcroft, M. K., Shaffrey, L., Black, E., & Brayshaw, D. J. (2015). Extratropical cyclones and the projected decline of winter Mediterranean precipitation in the CMIP5 models. *Climate Dynamics*, *45*(7–8), 1727–1738. https://doi.org/10.1007/s00382-014-2426-8

Zappa, G., Hoskins, B. J., & Shepherd, T. G. (2015). The dependence of wintertime Mediterranean precipitation on the atmospheric circulation response to climate change. *Environmental Research Letters*, *10*(10), 104012. https://doi.org/10.1088/1748-9326/10/10/104012

Zappa, G., Shaffrey, L. C., Hodges, K. I., Sansom, P. G., & Stephenson, D. B. (2013). A multimodel assessment of future projections of North Atlantic and European extratropical cyclones in the CMIP5 climate models. *Journal of Climate*, *26*(16), 5846–5862. https://doi.org/10.1175/jcli-d-12-00573.1

Zappa, G., & Shepherd, T. G. (2017). Storylines of atmospheric circulation change for European regional climate impact assessment. *Journal of Climate*, *30*(16), 6561–6577. https://doi.org/10.1175/jcli-d-16-0807.1

Zscheischler, J., Martius, O., Westra, S., Bevacqua, E., Raymond, C., Horton, R., et al. (2020). A typology of compound weather and climate events. *Nature Reviews Earth & Environment*, *1*, 333–347. https://doi.org/10.1038/s41467-020-15665-3